

Wall-to-bulk mass transfer in bubble columns with string of cones

M. Vijay¹
K.V. Ramesh²

Abstract

In the present study electrochemical reactions are carried out in bubble columns for achieving enhanced mass transfer rates. The mass transfer coefficient was computed from measured limiting currents at the electrodes fixed flush with the inner surface of the perspex tube wall which acted as test section. A string of cones arranged concentrically on a rod was used as the turbulent promoter. Improvements in the mass transfer coefficient due to cone elements are 100% when compared with the bubble column without any promoter. In the present study the effect of pertinent dynamic variables such as superficial gas velocity and liquid velocity; and geometric variables such as cone diameter, pitch, half apex angle of cone and rod diameter on mass transfer coefficient have been analyzed graphically. Correlation equations that gave best fit were obtained from least squares regression analysis, which can be used for the prediction of mass transfer coefficient.

Keywords:

Mass transfer coefficient;
Bubble column;
Augmentation;
Turbulent promoter.

Author correspondence:

M. Vijay,
Department of Chemical Engineering
Centurion University,Paralakhemundi, Gajapati, Odisha-India

1. Introduction (12pt)

A vast number of chemical process industries need to incorporate multiphase contactors in their process operations. Multiphase contactors are generally employed to carryout reactions that involve gas and liquid phases for the advantage of mass transfer. Gas-liquid upflow bubble columns are used in which thorough mixing occurs within the conduit due to bubble flow. Therefore isothermal conditions and uniform concentrations can be realized. In this regard potential applications are there for gas-liquid upflow bubble columns in process industries. Further, for achieving higher heat and mass transfer rates, turbulent promoters are employed. Magnitudes of enhancement in heat and mass transfer rates have been realized due to turbulence promoters in homogeneous liquid flow [1], liquid-solid fluidized beds [2], gas-liquid upflow bubble columns [3] and three-phase fluidized beds [4]. A close examination of literature revealed that a good number of works on augmentation of heat transfer and mass transfer were focused on employing displaced promoters in homogeneous flow and in fluidized beds. However, employing such promoters in gas-liquid flow systems are less in number. Promoters such as helicoidal tapes [5], disc promoters [6], twisted tapes [7], inclined discs [8], strings of spheres [9] and strings of hourglasses [3] were used in gas-liquid up flow bubble columns for realizing higher mass transfer coefficients. It was observed that Coaxially Placed Cones on a Rod (CPCR) internal in which a string of double cone elements were arranged concentrically on a rod yielded significant improvements in mass transfer in homogeneous flow and liquid-solid fluidized beds [10]. In view of this, for the present investigation it has been chosen to study, liquid-wall mass transfer in the presence of a string of cones internal in gas-liquid up flow bubble columns.

¹Department of Chemical Engineering, Centurion University, Paralakhemundi-761211, India.

²Department of Chemical Engineering, Andhra University, Visakhapatnam-530003, India.

2. Experimental

The aim of the present investigation is to obtain liquid-wall mass transfer coefficient in a gas-liquid up flow bubble column and a three-phase fluidized bed electrochemical reactor, both in the presence of coaxially placed string of cones promoter internal. The schematic of the experimental setup used in the present investigation was shown in Fig.1. The equipment and apparatus consisted of a storage tank (S), centrifugal pump (P), two rotameters (R_1 and R_2) and a nitrogen cylinder (N) along with regulator (R). A U-tube manometer (U) was provided to measure the pressure difference across the test section (B). Valves V_1 to V_5 were used to control the flow rate of liquid electrolyte through the experimental column where as V_6 and V_7 were employed to regulate the flow rate of nitrogen gas.

The storage tank was of 100 liters capacity, completely covered with a lid to avoid the contact between the electrolyte and the surrounding atmosphere. The bottom side of the tank was connected to the suction side of the pump (P) through a globe valve (V_1). A gate valve (V_2) was provided at the bottom of the storage tank to facilitate the periodic cleaning. The pump (P) of Kirloskar make was made of stainless steel that has a capacity of 1 kW. The discharge end of the pump was made into two sections, one directly connected to rotameter (R_1) and the other to a by-pass line.

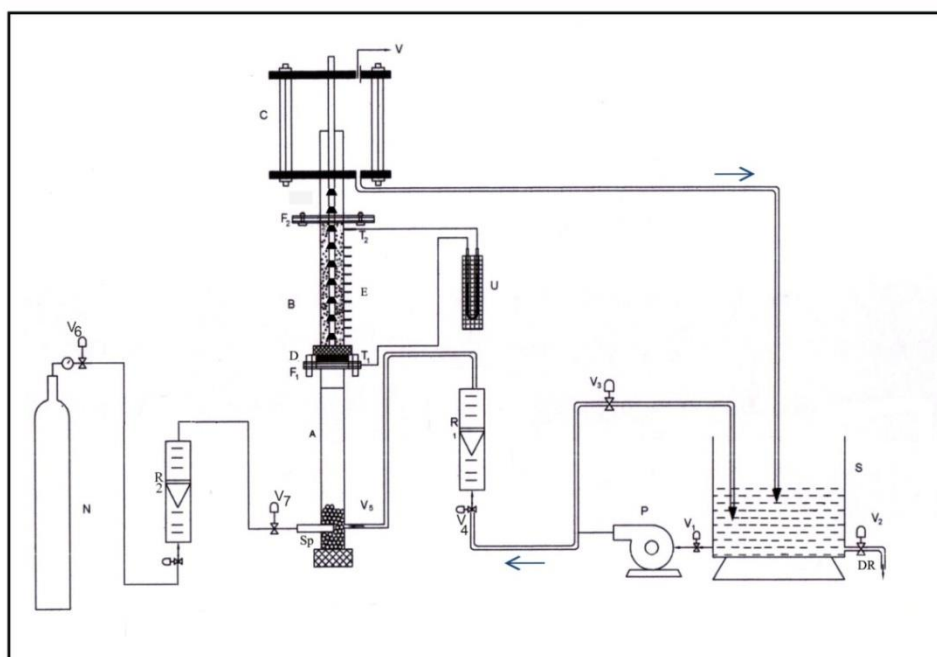


Fig.1: Schematic diagram of the experimental unit.

A - entrance calming section; B- test section; C- exit section; D-distributor wire mesh; DR- drain; E- electrodes; F_1 , F_2 - flanges; N- nitrogen cylinder; P-pump, R – Regulator, R_1 and R_2 – rotameters; S – storage tank; T_1 , T_2 - pressure tapings,U- manometer; V- vent; V_1 to V_7 - valves.

The by-pass line was provided with a globe valve V_3 to control the flow through rotameter. The rotameter (R_1) was of Indus make has range of 0 to 60 liters per minute for liquid flow. One more valve V_4 was provided at the entry point of liquid rotameter. Valve V_5 provided at the discharge end of the rotameter that facilitated the fluid electrolyte to flow through the experimental column.

AR grade nitrogen (IOLAR nitrogen) was procured from Bharat Oxygen Corporation, Visakhapatnam in high pressure cylinders. The cylinder was equipped with Nitrogen gas regulator. Precision regulator Model No. 316L of Concoa (France) make has been used as the gas regulator. For measurement of gas flow rate rotameter R_2 was used. This rotameter was of Indus make and has a pre calibrated range of 0 to 30 liters per min of nitrogen gas. Valve V_6 is provided at the entry point of rotameter R_2 while valve V_7 which was a needle valve that was arranged at the entry point of the experimental column.

The experimental column mainly consisted of three sections: an entrance calming section (A), a test section (B) and an exit section (C). The entrance calming section (A) was made of a copper tube of 6.73 cm inner diameter, outer diameter of 7.62 cm and 1.07 m long was filled with marble stones of random size. This leads to the elimination of tangential entry effects. This section was connected to the main test section (B) by means of a flange (F_1). The test section (B), which was the electrochemical cell, was made of smooth perspex tube of 6.73 cm inner diameter and 0.6 m height. Two inlets were provided in the bottom allowing the metered

gas and electrolyte to flow through the column. A stainless steel sparger (SP) was connected to the gas inlet to ensure uniform distribution of gas. The calming section was connected to the test section by means of a flange (F₁).

The inner wall of the test section was equipped with copper point electrodes 34 in number having a diameter of 3.42 mm. One end of these electrodes was fixed flush with inner surface of the test section while the other end projected outward served as terminal for connecting the electrodes to the external electric circuit. A stainless steel wire mesh placed at the bottom of the test section. This serves as fluid distributor (D) that supported the solid bed and also facilitated uniform distribution of electrolyte and gas. Two pressure taps, (T₁) and (T₂) were provided across the test section for pressure drop measurements. These taps were connected to the limbs of the U-tube manometer to measure the pressure drop. The U-tube manometer filled with CCl₄ as manometric liquid. The stainless steel wire mesh (D) also served as a supporter to hold the promoter element. The local limiting current was measured at the copper microelectrodes (0.00342 m diameter) fixed flush with the inner surface of the perspex test section. The electrical connectivity to the microelectrodes was checked using a digital multimeter. The exit calming section was a gas-liquid separator.

String of cones placed concentrically on a rod essentially acted as promoter internal in the present experimental studies. The schematic of the string of cones promoter assembly is shown Fig.2. The promoter elements of different geometric characteristics viz., diameter of rod (d_r), pitch (p), diameter of the base of the cone (d_c) and half of the apex angle (θ) were fabricated and used. The exit section was connected to the test section with a flange (F₂). The exit section (C) was also of the same diameter as A and B with its open end into the atmosphere. The gas liquid separator was provided with an open end to vent the nitrogen gas into the atmosphere and the electrolyte was drained into the storage tank from the bottom of the separator.

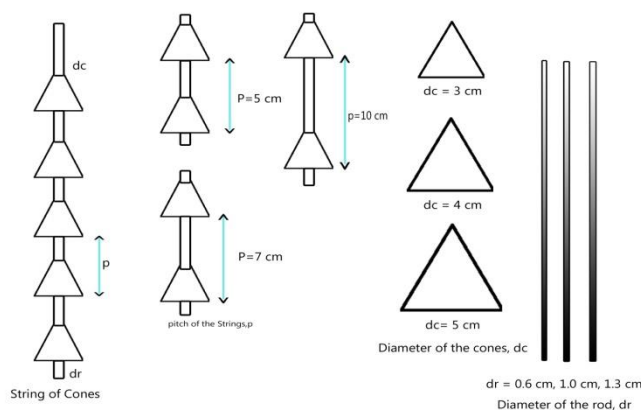
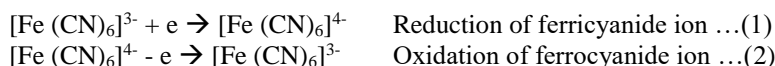


Fig.2. Details of the regular cone promoter variations

The limiting current was measured at copper point electrodes fixed flush with the inner surface of the test section. The diameter of point electrodes is 0.00324 m. The system chosen for the measurement of limiting current is potassium ferricyanide - ferrocyanide redox couple. The limiting current is measured for both the reduction of ferricyanide ion and oxidation of ferrocyanide ion. The electrode reactions involved in this study are:



80 liters of distilled water having a specific conductance less than 5 μS/cm were taken in the storage tank. Potassium ferricyanide, potassium ferrocyanide and sodium hydroxide were added to the distilled water in calculated quantities in such a way that the resulting electrolyte solution was an equimolar mixture (0.01 M) of potassium ferricyanide and potassium ferrocyanide with an excess indifferent electrolyte of 0.5M NaOH. The concentrations of ferrocyanide and ferricyanide ions were analyzed for each run. The ferrocyanide ion concentration was determined by permanganometry, ferricyanide ion concentration by iodometry. In all the runs the ferrocyanide and ferricyanide ion concentrations were maintained at 0.01M by periodical makeup.

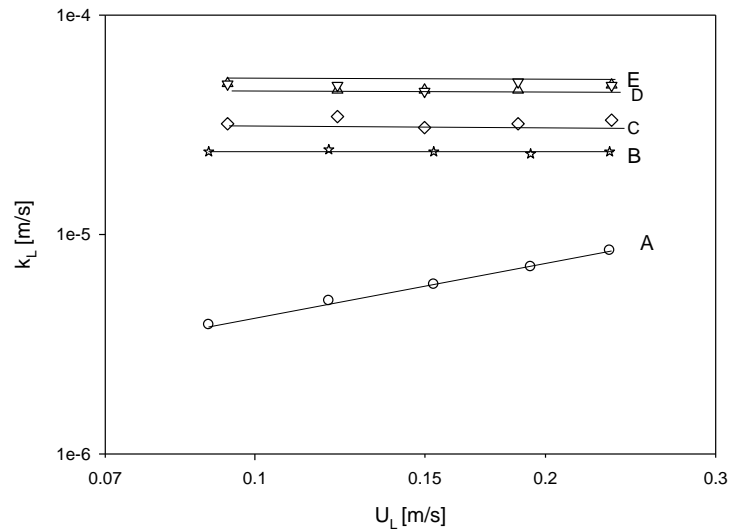
Measurement of limiting current was made in the lines similar to those reported earlier in the studies on ionic mass transfer [5]. From the measured limiting current value (i_L) at any given electrode, the mass transfer coefficient was calculated using the following equation.

$$k_L = \frac{i_L}{zAFC_0} \quad \dots (3)$$

3. Results and discussion

Initially, the wall-liquid mass transfer coefficient data were obtained in homogeneous flow in the presence of string of double cones as the promoter internal. Coulbrn j-factor j_D was computed from the experimental data on mass transfer. From the equations of SarveswaraRao [10], j_D data were also computed. A comparison of present experimental j_D data with that of predicted data reveals that the present experimental data obtained in homogeneous flow of electrolyte were in good agreement with that of SarveswaraRao [10].

Fig.3 gives the data of the present study plotted as mass transfer coefficient k_L against liquid velocity U_L for five cases of (i) homogeneous liquid flow (Plot A), (ii) gas-liquid up flow bubble column without any promoter element (Plot B), (iii) gas-liquid upflow bubble column with double cone promoter element (Plot C) (iv) gas-liquid up flow bubble column with regular cone promoter element (Plot D) and (v) gas-liquid upflow bubble column with inverse cone promoter element (Plot E). Plots B to E were obtained with superficial gas velocity maintained at 2.34 cm/s. The magnitudes of improvements over homogeneous liquid flow are shown through plots B, C, D and E. Plot A is the data predicted from Lin et al [11] for the case of homogeneous liquid flow (empty conduit flow) and plot B for the gas-liquid upflow bubble column without any promoter internal in accordance with Ramesh et al [5]. The plots C to E represent the present experimental mass transfer coefficient data in gas-liquid upflow bubble columns in the presence of conical promoters viz., doublecone, regular cone and inverse cone respectively. Plots A and B show that the improvements in the mass transfer coefficients due the introduction of doublecone internal in an otherwise homogeneous flow were upto a maximum of 2 fold. When inert nitrogen gas is introduced to the situation described by case A, the resulting flow system is the gas-liquid upflow bubble column represented by plot B. Examination of plots A and B reveals that the addition of gas yielded an enhancement in mass transfer coefficient at lower liquid velocity end upto 5 fold and as the liquid velocity goes on increasing, the enhancement gradually decreased and finally reached 2 fold on the higher velocity end within the range of liquid velocities considered in the present investigation. Therefore, the addition of gas phase yielded significant enhancement in mass transfer coefficient. Plot C gives the magnitudes of augmentation in limiting current density in two-phase gas-liquid upflow bubble column due to the introduction of doublecone promoter in which the enhancements were upto 40 percent over gas-liquid upflow bubble column without any promoter (Plots C and B). Similarly the augmentation in mass transfer coefficient due to theregular cone is 100 percent (Plots D and B); and inverse cone is also 100 percent (Plots E and B). The plots thus reveal that reckonable enhancement in mass transfer coefficient could be realized with string of cones promoter. Depending on the geometry of the conical element the augmentation varied from a minimum of 40 percent to 100 percent. One can reason that the conical promoter elements yield significant augmentation of mass transfer coefficient value.



System	d _r (mm)	d _c (cm)	p(cm)	U _g (m/s)	d _p (mm)	θ	plot
○ L	-----	-----	-----	-----	-----	-----	A
★ L+G	----	-----	-----	-----	-----	-----	B
△ L+G	10	4	5	0.0234	-----	45	E
▽ L+G	10	4	5	0.0234	-----	45	D
◇ L+G	10	4	5	0.0234	-----	45	C

Fig.3. Augmentation of mass transfer coefficient with liquid velocity in gas-liquid upflow bubble columns in the presence of different conical elements.

3.1. Axial variation of limiting current and mass transfer coefficient

In the present study with gas-liquid upflow bubble columns, the fluids flow upward in the test section in the presence of regular cone promoter element. Therefore, along the length of the test section, the flow area would be subjected to a series of contractions and expansions. One can reason that there appears varied turbulent intensity along the test section in the axial direction. This leads to fluctuating limiting current value in the longitudinal direction. In case of doublecone promoter element high fluctuations in limiting current have been reported by SarveswaraRao [10] in homogeneous flow. Therefore, in the present case also one can expect the fluctuating behavior of limiting current along the test section. Although the fluctuating behavior is seen, in the present case, with regular cone promoter element, the intensity of fluctuation is somewhat moderate and fell within ±19% which can be seen from Fig.4.

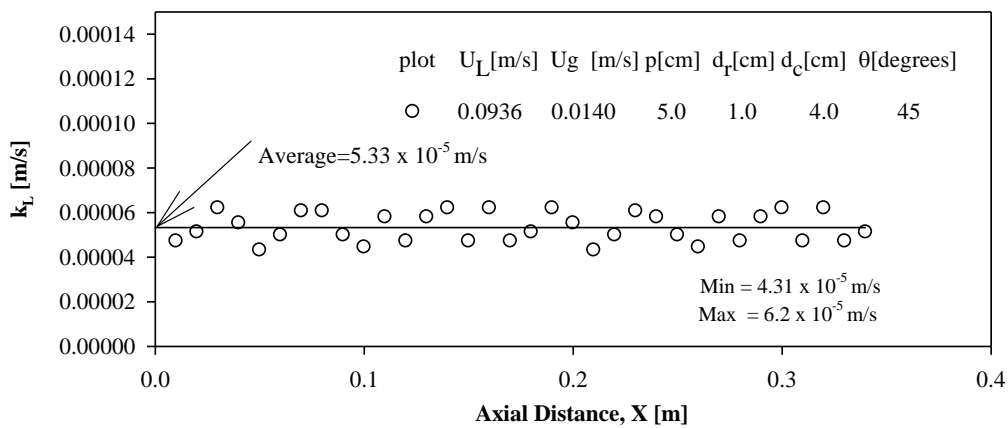


Fig.4. Longitudinal variation of mass transfer coefficient

3.2. Effect of liquid and gas velocities

It is well known that the liquid velocity was a very significant parameter in the case of homogenous flow either in empty conduit flow or with the doublecone promoter [10]. In gas-liquid upflow bubble columns without any promoter internal Ramesh et al [5] reported that the mass transfer coefficients were strongly influenced by the gas velocity and an increase in gas velocity resulted in increased mass transfer coefficient. The increase in the mass transfer coefficient due to the introduction of a small amount of gas into stationary liquid is by 10 fold and is extremely significant [5]. In the present study mass transfer coefficient data were obtained in a gas-liquid upflow bubble column in the presence of regular cone promoter $\{p = 5 \text{ cm}; d_r = 1 \text{ cm}; d_c = 4 \text{ cm}; \theta = 45^\circ\}$ at three different gas velocities and shown presented in Fig.5. The superficial gas velocities employed are 0.014, 0.023 and 0.037 m/s respectively.

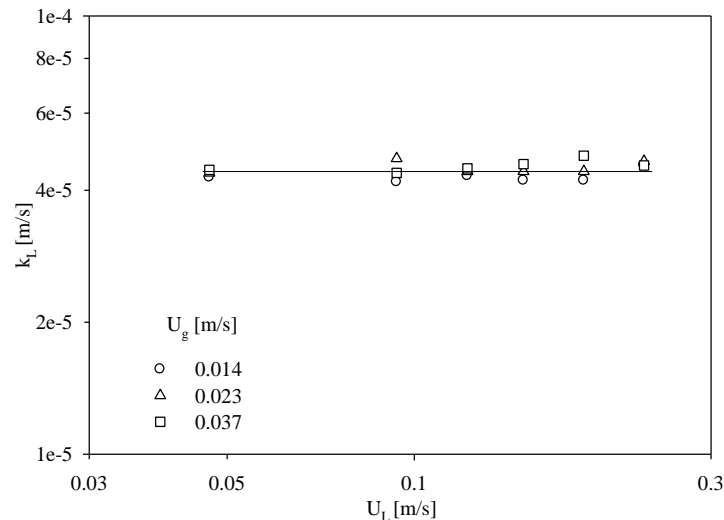


Fig.5. Effect of gas velocity on k_L at constant $p=5 \text{ cm}$, $d_r= 1 \text{ cm}$, $d_c= 4 \text{ cm}$, $\theta=45^\circ$

It is clearly seen from the plots of the figure that both the liquid and gas velocities have not exhibited any noticeable effect on the mass transfer coefficient in gas-liquid two-phase upflow bubble column in the presence of regular cone promoter internal. The reason for this can be attributed to the overall turbulence generated by the gas phase, liquid phase and promoter internal which was very large so that the turbulence coming out of the variations in gas and liquid velocities was insignificant. This observation is also conspicuous from Fig.6 which was drawn between mass transfer coefficient and gas velocity for three different liquid velocities viz., 0.0936, 0.1214 and 0.1498 m/s.

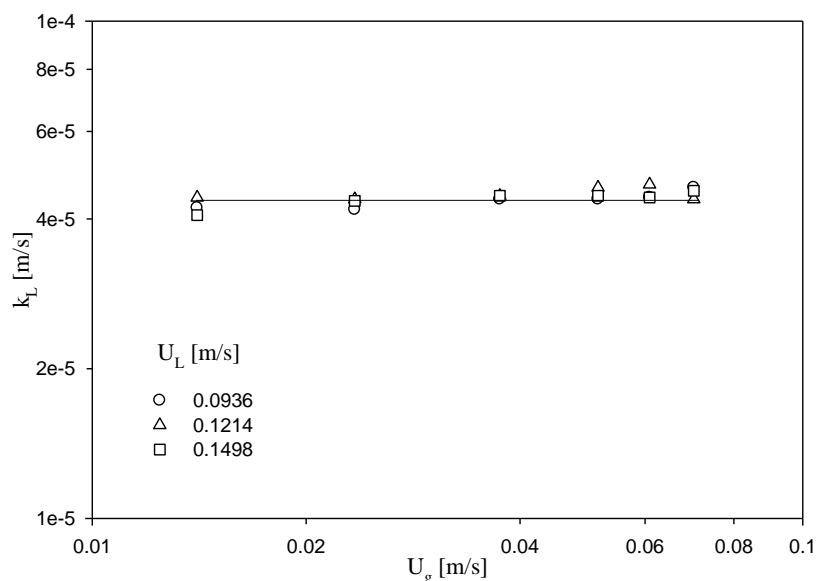


Fig.6: Effect of liquid velocity (U_L) on k_L at constant $p=5 \text{ cm}$, $d_r= 1 \text{ cm}$, $d_c= 4 \text{ cm}$, $\theta=45^\circ$

3.3. Effect of pitch

Fig.7 shows the mass transfer coefficient data obtained for the case of a regular cone promoter element $\{d_r = 1 \text{ cm}; d_c = 4 \text{ cm}; \theta = 45^\circ\}$ against liquid velocity for three different pitch values viz., 5, 7 and 10 cm at a constant superficial gas velocity of 0.0234 m/s. A close examination of the plots of this figure reveals that higher k_L values were realized for lowest pitch and as the pitch was

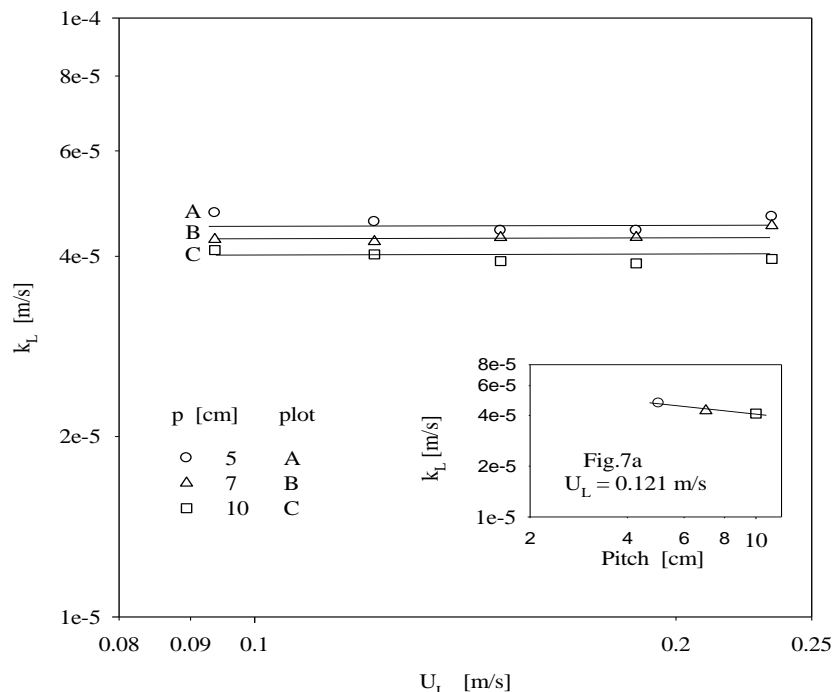


Fig.7. Effect of pitch: Variation of k_L with U_L at constant $U_g = 0.0234 \text{ m/s}$. $\{d_r = 1 \text{ cm}, d_c = 4 \text{ cm}, \theta = 45^\circ\}$

increased the k_L values decreased. It is well understood that the main resistance to the mass transfer was the resistance film that appears on the electrode surface. In the case of lower pitch value, the test section is occupied with more number of regular cone promoter elements and as the fluids flow past these objects, the fluids are subjected to more number of contractions and expansions in the cross section. This leads to increased turbulence in the fluid electrolyte. This results in great reduction in the thickness of the resistance film. Thus higher mass transfer coefficient values were realized. As the pitch value is increased, the number of elements that present in the test section gets reduced. Therefore, the number of times the fluids get exposed to sudden contractions and expansions also come down. Hence the turbulence that generates out of this becomes less. Therefore, there would be a reduction in values of the mass transfer coefficient that occurs at the electrode surface. Hence lower values of mass transfer coefficient can be expected with increase in pitch. The inset figure Fig.7a is also in accordance with the reasoning presented.

3.4. Effect of rod diameter

The mass transfer coefficient data obtained for the case of a regular cone promoter element $\{p = 7 \text{ cm}; d_c = 4 \text{ cm}; \theta = 45^\circ\}$ were plotted against superficial gas velocity for three different rod diameters viz., 0.6, 1.0 and 1.3 cm at a constant superficial liquid velocity of 0.121 m/s and is shown in Fig.8. A close look at the plots of this graph indicates that the points fell closely indicating that the influence of rod diameter on mass transfer coefficient is relatively insignificant. The promoter rod is placed coaxially at the center of the column. When the flow is taking place, presence of regular cone is likely to lead to the formation of sudden contractions and expansions, resulting in turbulence. The promoter rod diameter being small in comparison with the column diameter, the change in local fluid velocities due to the presence of the promoter rod is marginal. Hence, the average mass transfer coefficient is not likely to be affected by promoter rod diameter.

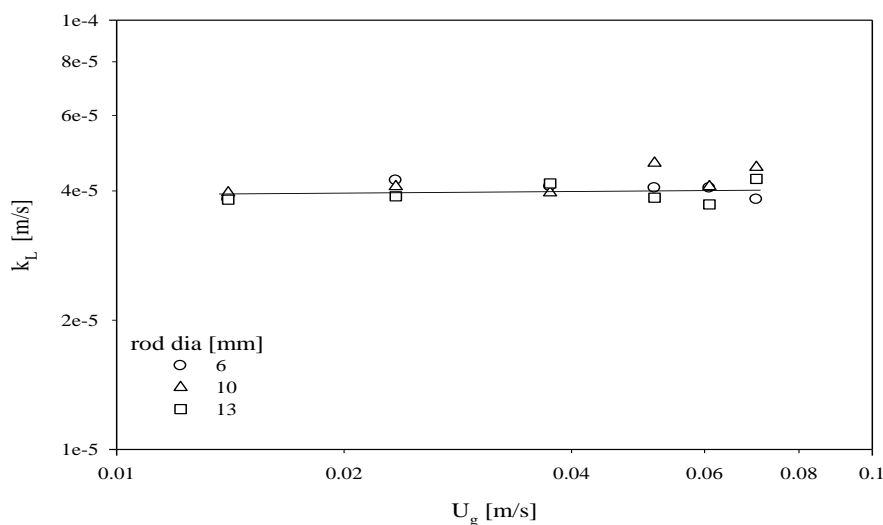


Fig.8. Effect of rod diameter: Variation of k_L with U_g at constant $U_L = 0.121$ m/s
{ $p = 7$ cm; $d_c = 4$ cm; $\theta = 45^\circ$ }

3.5. Effect of cone diameter

Fig.9 shows the mass transfer coefficient data obtained for the case of a regular cone promoter element { $p = 7$ cm; $d_r = 1$ cm; $\theta = 45^\circ$ } against liquid velocity for three different cone diameter values viz., 3, 4 and 5 cm at a constant superficial gas velocity of 0.0234 m/s. A close inspection of the plots of this figure indicates that higher k_L values were realized for highest cone diameter and as the cone diameter was increased the k_L values increased. One is well aware that the main resistance to the mass transfer was the resistance film that forms on the electrode surface. In the case of higher cone diameter, a maximum cross section of the test section is occupied with regular cone promoter element and as the fluids flow past this object, the fluids have to pass through smaller area available between the column wall and the regular cone element. Hence the local velocities of the fluids increase sharply. This phenomenon leads to increased turbulence in the fluid electrolyte. This results in great reduction in the thickness of the resistance film. Thus higher mass transfer coefficient values were realized. As the cone diameter value is decreased, the area available for flow of the fluids would increase and hence, the local velocities of the fluids decrease. Therefore the turbulence that generates out of this becomes less. Therefore, there would be a reduction in values of the mass transfer coefficient that occurs at the electrode surface. Hence lower values of mass transfer coefficient can be expected with decrease in cone diameter. The inset figure Fig.9a is also in accordance with the reasoning presented.

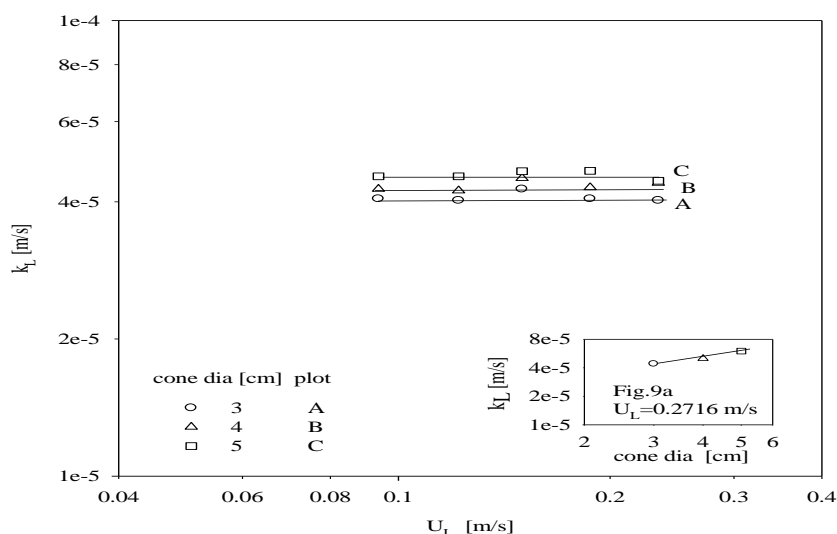


Fig.9. Effect of cone dia: Variation of k_L with U_L at constant $U_g = 0.0234$ m/s
{ $p = 7$ cm; $d_r = 1$ cm; $\theta = 45^\circ$ }

3.6. Effect of half apex angle of cone

Fig.10 shows the mass transfer coefficient data obtained for the case of a regular cone promoter element {p = 7 cm; d_r = 1 cm; d_c = 4 cm} against liquid velocity for three different half cone-apex-angle values viz., 30, 45 and 60° at a constant superficial gas velocity of 0.0234 m/s. A close examination of the plots of this figure indicates that higher k_L values were realized for highest cone angle and as the cone angle was increased the k_L values also increased.

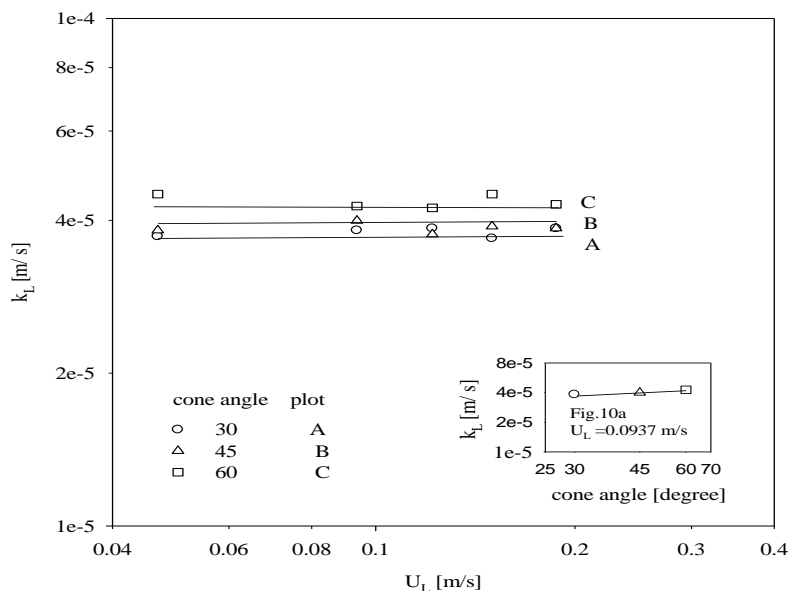


Fig.10. Effect of cone angle: Variation of k_L with θ at constant U_g = 0.0234 m/s. {p = 7 cm; d_r = 1cm; d_c = 4 cm}

It can be understood that smallest cone angle refers to more streamlined configuration and highest cone angle refers to more bluff body configuration. It is already established that the streamlined bodies generate unseparated boundary layers whereas the bluff bodies generate separated boundary layers. Further it is very clear that in the case of unseparated boundary layers the turbulence intensity is small and in the case of separated boundary layers the turbulent intensity is more. Therefore it can be reasoned that less angle yields lower mass transfer coefficient and high angle yields higher mass transfer coefficient. As per the mechanism discussed, an increase in cone angle should result in an increase in mass transfer coefficient. The trends exhibited by the plots of Fig.10 also in accordance with the above mentioned mechanism. The increasing mass transfer coefficient with increasing cone angle is also evident from the inset Fig.10a.

3.7. Correlation

The entire data on mass transfer coefficient obtained in the present investigation was correlated by regression analysis which yielded the following equation:

$$j_D = 154.6 (Re_L)^{-0.92} (Frg)^{0.016} \left(\frac{p}{D_c}\right)^{-0.15} \left(\frac{d_c}{D_c}\right)^{0.15} \left(\frac{d_r}{D_c}\right)^{0.02} (1 + \sin \theta)^{0.21} \dots (3)$$

Average deviation = 4.483 percent
Standard deviation = 6.375 percent

In eqn. (3) the exponents on Fr_g and (d_r/D_c) are very small. Hence these two terms can be eliminated from this equation. Further the terms (p/D_c) and (d_c/D_c) have the same value of exponent with different signs, both them can be combined into one term. Then the resulting equation is

$$j_D = 142.6 (Re_L)^{-0.92} \left(\frac{d_c}{p}\right)^{0.15} (1 + \sin \theta)^{0.21} \dots (4)$$

Average deviation = 4.770 percent
Standard deviation = 6.520 percent

The correlation factor Y is defined as

$$Y = j_D \left(\frac{d_c}{p}\right)^{-0.15} (1 + \sin \theta)^{-0.21} \dots (5)$$

A correlation plot has been drawn by taking Y on Y-axis and Re_L on X-axis. The plot thus obtained is shown presented in Fig.11.

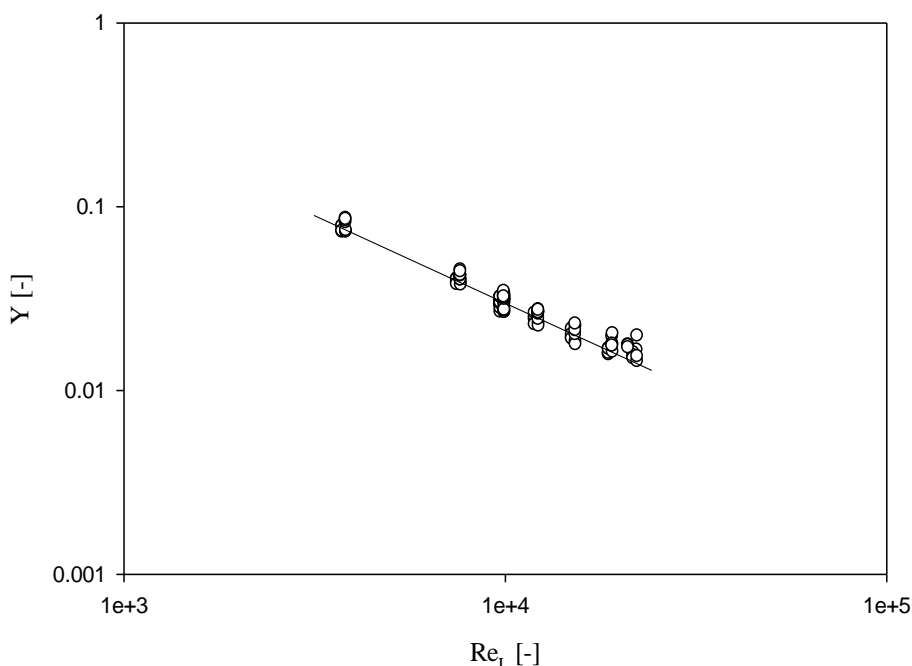


Fig.11. Correlation plot in accordance with eqn.(4)

4. Conclusion

Experimental investigation was carried out to study the influence of various dynamic and geometric variables in an electrochemical cell on liquid to wall mass transfer coefficient both in two-phase bubble columns and in three-phase fluidized beds in the presence of a coaxially placed string of cones promoter element. Regular cone is employed as repeating elements. Limiting current measurements were obtained at point copper electrodes fixed flush with inner wall of the electrochemical cell.

The limiting current data for the cases of reduction of ferricyanide ion and oxidation of ferrocyanide ion were obtained for gas flow rates ranging from 5 to 25 m/s. The flow rate of electrolyte was varied from 16.7 m/s to 83.3 m/s. Coaxially placed string of cones promoter with different cone dimensions (d_c , p , θ , d_r) - for obtaining the data.

Based on about 3000 limiting current measurements both in phase bubble column, the data were analyzed for individual parametric effects and the following conclusions were drawn:

- (i) The improvements in mass transfer coefficients due to regular cone promoter in three bubble column were up to 100%.
- (ii) The mass transfer coefficient varied along the length of the test section in the flow direction and the fluctuations were within $\pm 20\%$ for three kinds of promoter elements employed in the present study.
- (iii) Variation in the mass transfer coefficients due to increase in liquid and gas velocities in the presence of string of cones is insignificant.

- (iv) In the presence of regular cone promoter, an increase in pitch caused a reduction in mass transfer coefficient.
- (v) In the presence of regular cone promoter, an increase in cone diameter and half-apex angle of cone caused an increase in mass transfer coefficient.
- (vi) The influence of rod diameter on mass transfer coefficient is found to be insignificant.

Nomenclature

A	= area of the reacting surface	[m ²]
C ₀	= concentration of ferricyanide ion	[kmol/m ³]
d _c	= characteristic length	[m]
D _c	= column diameter	[m]
D _L	= diffusivity of reacting ion	[m ² /s]
d _r	= diameter of the rod	[m]
F	= Faraday constant	[C/mol of electrons]
i _L	= limiting current	[A]
k _L	= local mass transfer coefficient	[m/s]
k _{L,avg}	= average mass transfer coefficient	[m/s]
p	= pitch	[m]
U _L	= superficial liquid velocity	[m/s]
U _g	= superficial gas velocity	[m/s]
n	= number of electrons released or consumed during the reaction	[-]

Dimensionless groups

$$Fr_g = \text{mass transfer factor} = \frac{U_g^2}{gD_c} \quad [-]$$

$$j_D = \text{mass transfer factor} = \frac{k_L}{U_L} Sc^{2/3} \quad [-]$$

$$Re = \text{Reynolds number} = \frac{\rho_L D_c U_L}{\mu_L} \quad [-]$$

$$Sc = \text{Schmidt number} = \frac{\mu}{\rho D_L} \quad [-]$$

Greek symbols

μ _L	= Viscosity of electrolyte	[Pa.s]
ρ _L	= density of the electrolyte	[kg/m ³]

References

1. G.V.S.K. Reddy, M. S.N. Murthy, B. Srinivas, K.V. Ramesh, Liquid-wall Mass Transfer in Homogeneous Flow with Coaxially placed String of Hemispheres, Journal of The Institution of Engineers (India) Series E 95(2) 69-74 (2014).
2. NiranjanaRao, B., Ramaprasad, B.S.G., Murthy, M.S.N., Ramesh K.V., Wall-to-Bed Mass Transfer in a Fluidized Bed Electrochemical Reactor in the Presence of Angled Disc Promoter, AIChE Spring Meeting & 11th Global Congress on Process Safety 2015/4/28.
3. S. Suresh, M.S.N. Murty, B. Srinivas, K.V. Ramesh, Wall-to-bulk mass transfer in concurrent gas liquid upflow bubble column using hourglass promoters, Journal of The Institution of Engineers (India) Series E 94(2) 91-96 (2013).
4. P. Rohini Kumar, K. Ashok Kumar, M.S.N. Murty, K.V. Ramesh, Wall-to-bed mass transfer in three-phase fluidized beds in the presence of angled disc promoter, Heat and Mass Transfer, (In press)
5. K.V. Ramesh, G.M.J. Raju, M.S.N. Murty, C. BhaskaraSarma, Wall-to-bulk mass transfer in a two-phase upflow bubble column with a composite promoter, Indian Chemical Engineer, 51 (3) 215-227 (2009).
6. G.V.S. Sarma, M.S.N. Murty, K.V. Ramesh, G.M.J. Raju, Wall-to-bulk mass transfer in gas-liquid

- upflow bubble column with disc promoter, *Journal of Energy Heat and Mass Transfer*, 33, 233-249 (2011).
7. B.S. Subramanyam, M.S.N. Murty, B. SurendraBabu, K.V.Ramesh, Wall-to-bulk mass transfer in a gas-liquid upflow bubble column with loose-fit twisted tape internals, in *Proceedings of International Conference on Advances in Chemical Engineering and Technology ICACE TKMCE '14*, October 16-18, Kollam, India. Pp .82-85 (Elsevier).ISBN 9789351072843
 8. B.S.G. Ramaprasad, B. NiranjanaRao, K. Ashok Kumar, K.V. Ramesh, Mass Transfer in a gas liquid upflow bubble column in the presence of angled disc promoter, *Chemical Technology: An Indian Journal* 11(5) 1 – 9 (2016).
 9. P. Rohini Kumar, K. Ashok Kumar, P. Venkateswarlu, K.V. Ramesh, Wall-to-bulk mass transfer in cocurrentupflow bubble column with coaxially placed string of spheres, *Am. J. Heat Mass Transfer* 3(4) 225-237 (2016).
 10. S. SarveswaraRao, Studies on ionic mass transfer with coaxially placed cones on a rod (CPCR internal) in homogeneous fluid and fluidized beds, Ph.D. thesis, Andhra University, Visakhapatnam, India (1983).
 11. C.S. Lin, E.B. Denton, H.S. Gaskill, C.L. Putnam, *Diffusion Controlled Electrode Reactions*, *Ind. Eng. Chem.*, 43, pp. 2136-2143 (1951).